Journal of the Serbian Chemical Society
JSCS-info@shd.org.rs • www.shd.org.rs/JSCS

ACCEPTED MANUSCRIPT

This is an early electronic version of an as-received manuscript that has been accepted for publication in the Journal of the Serbian Chemical Society but has not yet been subjected to the editing process and publishing procedure applied by the JSCS Editorial Office.

Please cite this article as D. Manasijević, *J. Serb. Chem. Soc.* (2026) https://doi.org/10.2298/JSC260821068M

This "raw" version of the manuscript is being provided to the authors and readers for their technical service. It must be stressed that the manuscript still has to be subjected to copyediting, typesetting, English grammar and syntax corrections, professional editing and authors' review of the galley proof before it is published in its final form. Please note that during these publishing processes, many errors may emerge which could affect the final content of the manuscript and all legal disclaimers applied according to the policies of the Journal.

Journal of the Serbian Chemical Society
JSCS-info@shd.org.rs • www.shd.org.rs/JSCS
J. Serb. Chem. Soc. **00(0)** 1-20 (2026)
JSCS–14148
Original scientific paper
Published DD MM, 2026

Accepted manuscript

Thermodynamic assessment of industrial pyrometallurgical extraction routes for refractory metals

DRAGAN MANASIJEVIĆ*

University of Belgrade, Technical Faculty in Bor, Bor, Serbia.

(Received 21 August; revised 6 November; accepted 9 November 2026)

Abstract: Industrial production of refractory metals is governed primarily by thermodynamic constraints arising from the strong affinity of these metals toward carbon and oxygen. In the present work, a unified thermodynamic assessment of representative refractory metals (V, Nb, Ta, Mo, W, and Re) was performed to establish the thermodynamic basis for selecting pyrometallurgical extraction routes. Standard Gibbs free energy calculations, Ellingham diagrams, and HSC Chemistry equilibrium calculations were employed to compare oxide stability, carbide formation tendency, hydrogen reduction, metallothermic reduction, and chlorination-based extraction routes. The calculations show that Nb_2O_5 and Ta_2O_5 possess the highest thermodynamic stability and simultaneously exhibit the strongest tendency toward carbide formation, explaining why chlorination followed by metallothermic reduction is preferred industrially. In contrast, MoO_3 and WO_3 are sufficiently reducible by hydrogen, while equilibrium calculations demonstrate the important influence of hydrogen excess on the final metallization degree. Metallothermic reduction of V_2O_5 with Al, Mg, and Ca is thermodynamically feasible over the investigated temperature range, whereas industrial preference for aluminothermy is mainly determined by technological and economic factors. Thermodynamic analysis of chlorination and carbochlorination further demonstrates that direct chlorination of Nb_2O_5 and Ta_2O_5 is unfavorable, while carbochlorination provides a strong driving force for pentachloride formation. The results provide a consistent thermodynamic explanation for the selection of industrial extraction routes for refractory metals.

Keywords: Ellingham diagrams; Gibbs free energy; equilibrium calculations; hydrogen reduction; carbochlorination; metallothermy.

INTRODUCTION

Refractory metals constitute a technologically important class of engineering materials owing to their extremely high melting temperatures, excellent high-temperature strength, superior thermal conductivity, good corrosion resistance,

* Corresponding author. E-mail: dmanasijevic@tfbor.bg.ac.rs
https://doi.org/10.2298/JSC260821068M

and significant stability under severe service conditions. These unique properties have enabled their widespread application in aerospace propulsion, nuclear energy systems, high-temperature furnaces, chemical processing equipment, electronics, defense technologies, and advanced energy conversion systems. In recent years, the growing demand for high-performance materials capable of operating under increasingly extreme conditions has further stimulated research into refractory metals and their extraction, processing, and recycling.[1-5]

Despite their extensive industrial importance, the definition of refractory metals is not entirely consistent throughout the literature. Some authors classify refractory metals as metallic elements with melting temperatures exceeding approximately 1650 °C, thereby including Ti, Zr, Hf, Cr, V, Nb, Mo, Ta, W, and Re.[2] In contrast, many contemporary publications adopt a more restrictive definition based on melting temperatures above 2000 °C and primarily consider V, Nb, Ta, Mo, W, and Re as the representative refractory metals.[1,5] Regardless of the adopted classification, all these metals exhibit very high thermal stability and present considerable challenges during extractive metallurgy.

The extraction of refractory metals differs substantially from that of common engineering metals because their oxides possess high thermodynamic stability, while several of these metals readily form stable carbides or oxycarbides during carbothermic reduction.[6,7] Consequently, conventional pyrometallurgical reduction routes are often ineffective or produce impure products. Industrial production therefore relies on various alternative technologies, including hydrogen reduction, metallothermic reduction, and chlorination followed by chloride reduction.[8-12] The selection of a particular extraction route is fundamentally governed by thermodynamic constraints rather than solely by technological considerations. Although hydrometallurgical and electrometallurgical technologies also play important roles in the production and purification of refractory metals, particularly for niobium and tantalum, the present study is restricted to pyrometallurgical routes whose feasibility is governed primarily by high-temperature thermodynamics.

Even though numerous review papers discuss the processing, alloy design, additive manufacturing, and applications of refractory metals, systematic thermodynamic comparisons explaining why different industrial extraction routes are required for individual refractory metals remain relatively scarce. In particular, a unified assessment of oxide stability, reduction behavior, carbide formation tendency, chlorination reactions, and equilibrium phase relationships has not been comprehensively presented.

Therefore, the objective of the present work is to establish a unified thermodynamic framework for evaluating the extraction behavior of representative refractory metals (V, Nb, Ta, Mo, W, and Re). Gibbs free energy calculations, Ellingham diagrams, and equilibrium calculations performed using HSC

Accepted manuscript

Chemistry software are employed to compare the thermodynamic feasibility of carbothermic, hydrogen, metallothermic, and chlorination-based extraction routes. The obtained results provide a consistent explanation for the industrial preference of different extraction technologies and identify the principal thermodynamic limitations controlling the production of refractory metals.

METHODOLOGY

The thermodynamic calculations were performed using HSC Chemistry software (ver. 10.8.2.0).[13] Standard Gibbs free energy changes were calculated using the Reaction Equations module, while equilibrium phase compositions were determined by Gibbs free-energy minimization using the Equilibrium Compositions module. Ellingham diagrams were constructed for oxide formation reactions normalized to one mole of oxygen, whereas carbide formation reactions were normalized to one mole of carbon to enable direct comparison of thermodynamic stability. Hydrogen reduction, metallothermic reduction, chlorination, carbochlorination, and chloride-reduction reactions were evaluated under standard-state conditions. Equilibrium calculations were performed at a total pressure of 1 bar using stoichiometric and excess amounts of reducing agents depending on the investigated process. All relevant condensed and gaseous species available in the HSC thermodynamic database were included in the equilibrium calculations.

The calculated thermodynamic trends were interpreted in the context of published industrial extraction routes. Although rhenium is included in the comparative Ellingham analysis, subsequent sections focus on V, Nb, Ta, Mo, and W because the industrial recovery of rhenium is governed primarily by the volatility of Re_2O_7 during oxidative roasting rather than by the pyrometallurgical reduction routes considered in the present work.

RESULTS AND DISCUSSION

Thermodynamic stability of refractory metal oxides

Fig. 1 presents the Ellingham diagram for the oxidation of representative refractory metals together with the equilibrium lines for the C/CO, CO/CO_2 and H_2/H_2O systems. The Gibbs free energy changes were normalized to one mole of oxygen to enable direct comparison of oxide stability over the investigated temperature range.

The stability decreases in the following order:

$$Ta_2O_5 > Nb_2O_5 > V_2O_5 > WO_3 > MoO_3 > Re_2O_7$$

This trend is consistent with previously reported comparative Ellingham analyses of Group IV–VI refractory metal oxides.[14] Among the investigated oxides, tantalum pentoxide exhibits the lowest Gibbs free energy throughout the entire temperature range, indicating the highest resistance toward chemical reduction. Niobium pentoxide shows very similar behavior, reflecting the close chemical similarity between niobium and tantalum. In contrast, molybdenum and tungsten oxides are considerably less stable, while rhenium oxide exhibits the lowest thermodynamic stability.

Accepted manuscript

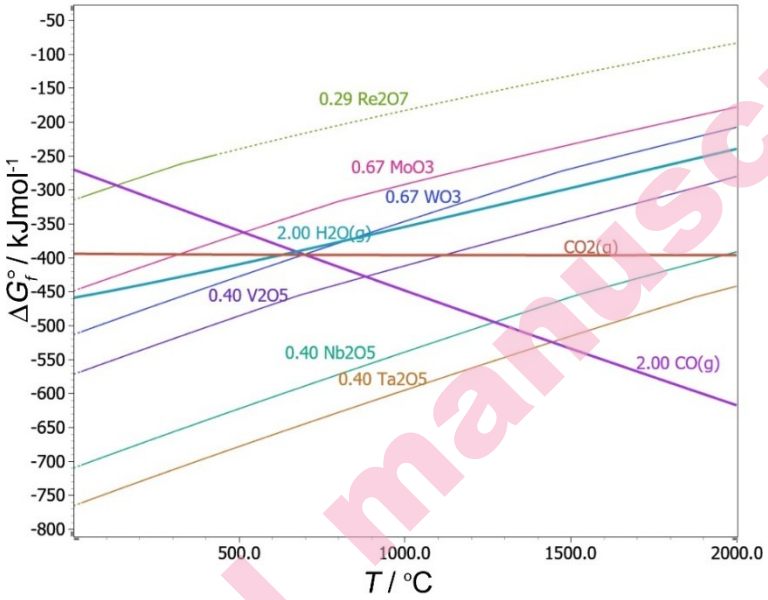


Fig. 1. Standard Gibbs energy changes for the formation of representative refractory metal oxides together with the equilibrium lines for common reducing agents (C and H_2). All reactions were normalized to one mole of O_2.

All oxide stability curves display positive slopes, indicating that oxide stability decreases with increasing temperature. Consequently, elevated temperatures thermodynamically favor oxide reduction, although the extent of this effect strongly depends on the intrinsic stability of each oxide.

Comparison with the H_2/H_2O equilibrium line reveals that molybdenum and tungsten oxides become thermodynamically reducible by hydrogen over a broad high-temperature region, whereas the reduction of Nb_2O_5 and Ta_2O_5 remains considerably less favorable. These results are fully consistent with industrial practice, where hydrogen reduction represents the principal production route for metallic molybdenum and tungsten powders, while niobium and tantalum are generally extracted via chlorination followed by metallothermic reduction.

A similar conclusion can be drawn from comparison with the carbon oxidation reactions. The large separation between the CO/CO_2 equilibrium lines and the stability curves of Nb_2O_5 and Ta_2O_5 demonstrates that direct carbothermic reduction is thermodynamically unfavorable. Vanadium pentoxide occupies an intermediate position between molybdenum/tungsten oxides and the highly stable oxides of niobium and tantalum, explaining why industrial vanadium production frequently relies on aluminothermic or calciothermic reduction, whereas carbothermic processes are mainly employed for ferrovanadium production rather than for obtaining high-purity metallic vanadium.

Accepted manuscript

The very low thermodynamic stability and high volatility of Re_2O_7 distinguish rhenium from the other refractory metals. Unlike Nb, Ta, Mo, and W, the volatility of rhenium oxide governs its industrial extraction, enabling efficient recovery of rhenium from roasting gases generated during molybdenite processing.[15]

Overall, the Ellingham analysis demonstrates that the industrial extraction routes of refractory metals are primarily governed by the thermodynamic stability of their oxides.[14] However, oxide stability alone cannot fully explain the limited applicability of carbothermic reduction. An equally important factor is the strong tendency of several refractory metals to form highly stable carbides, which is analyzed in the following section.

Thermodynamic stability of refractory metal carbides

Fig. 2 presents the standard Gibbs energy changes for the formation of representative refractory metal carbides from their constituent elements. All reactions were normalized to one mole of carbon to enable direct comparison of carbide stability over the investigated temperature range.

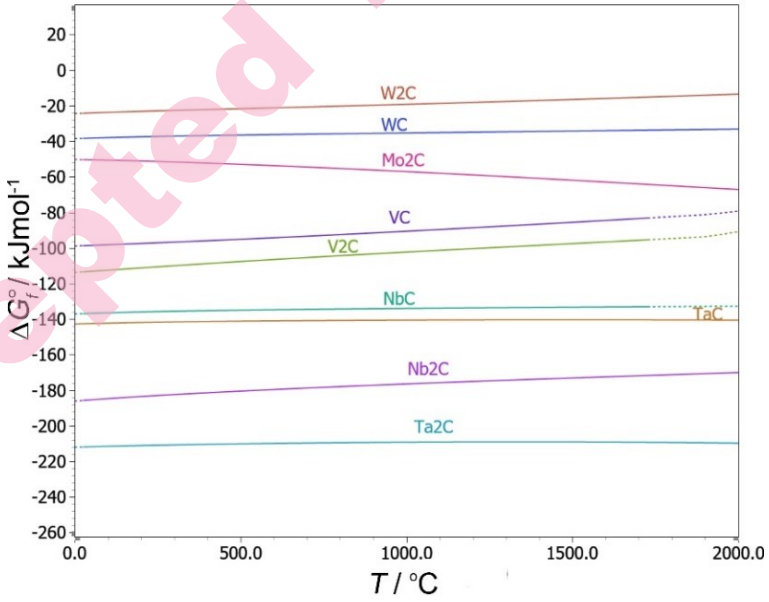


Fig. 2. Standard Gibbs energy changes for the formation of representative refractory-metal carbides from their constituent elements. All reactions were normalized to one mole of carbon.

The calculated Gibbs energy values remain negative throughout the investigated temperature range for all carbides, confirming the strong affinity of refractory metals toward carbon and the thermodynamic feasibility of carbide formation during carbothermic reduction.

Accepted manuscript

Among the investigated carbides, Ta_2C and Nb_2C exhibit the most negative Gibbs energy values, indicating the highest thermodynamic stability. These results agree well with previous thermodynamic assessments of group IVB and VB transition-metal carbides and explain why carbothermic reduction of Ta_2O_5 and Nb_2O_5 preferentially leads to carbide formation rather than high-purity metals.[16] Vanadium exhibits intermediate behavior, with both VC and V_2C remaining thermodynamically stable but less favorable than the corresponding tantalum and niobium carbides, consistent with the industrial preference for metallothermic production of metallic vanadium.[10]

In contrast, tungsten and molybdenum carbides exhibit considerably less negative Gibbs energy values. Consequently, hydrogen reduction can be successfully employed for the industrial extraction of tungsten and molybdenum powders while minimizing carbide formation under appropriately controlled processing conditions.

Comparison of Figs. 1 and 2 demonstrates that refractory metals forming the most stable oxides (Nb and Ta) also exhibit the strongest tendency toward carbide formation. Consequently, carbothermic reduction is hindered not only by the exceptional stability of their oxides but also by the simultaneous formation of highly stable carbides, providing a thermodynamic explanation for the industrial preference for chlorination followed by metallothermic reduction. Conversely, the lower stability of both oxides and carbides in the Mo–W systems makes hydrogen reduction the preferred industrial extraction route. These results demonstrate that the selection of pyrometallurgical extraction technologies is governed by the combined stability of both oxides and carbides rather than by oxide stability alone.

Equilibrium analysis of hydrogen reduction of molybdenum and tungsten oxides

The calculated equilibrium compositions during the hydrogen reduction of 1 kmol of MoO_3 and WO_3, respectively, using initial hydrogen amounts of 3, 4, and 5 kmol at a total pressure of 1 bar are presented in Figs. 3 a-c and 4 a-c. The selected hydrogen quantities correspond to the stoichiometric requirement for complete reduction and to progressively increasing hydrogen excess. The calculations demonstrate that both oxide systems are strongly affected by the initial hydrogen availability, although their reduction behavior differs considerably because of the different thermodynamic stability and complexity of the Mo–O and W–O systems.

Accepted manuscript

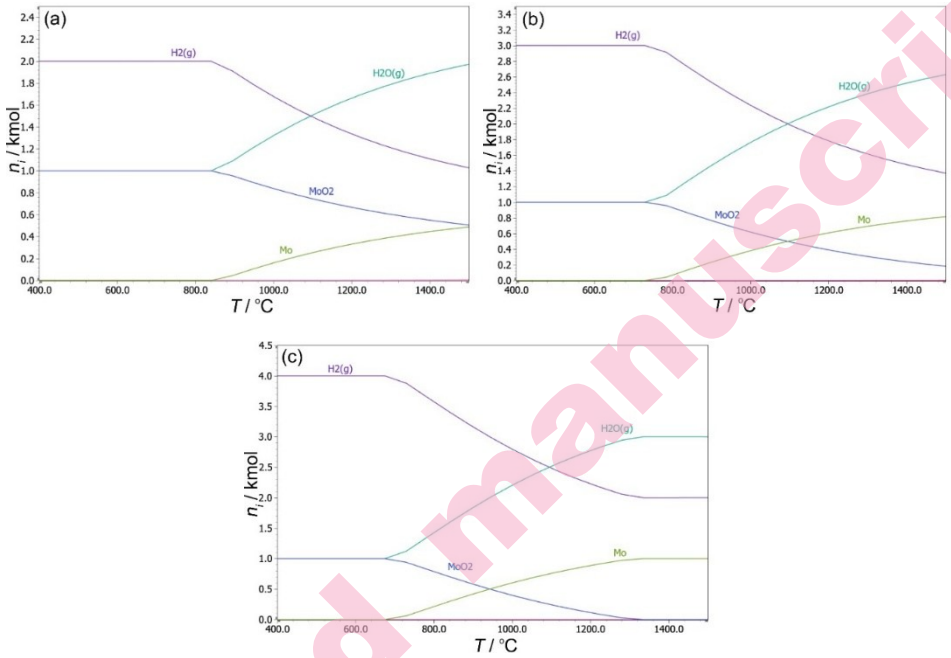


Fig. 3. Calculated equilibrium compositions during the hydrogen reduction of 1 kmol of MoO_3 with initial hydrogen amounts of (a) 3, (b) 4, and (c) 5 kmol at a total pressure of 1 bar.

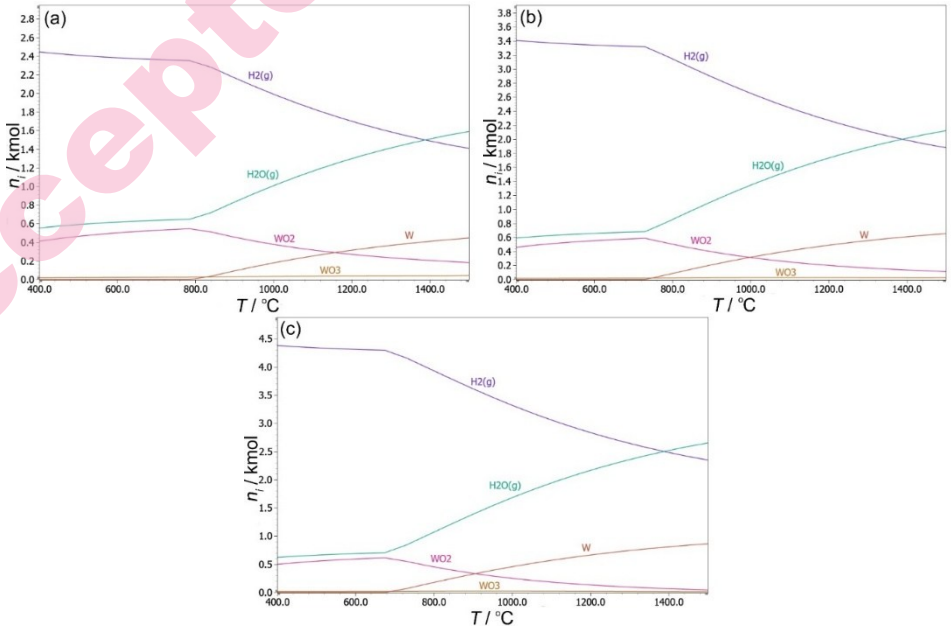


Fig. 4. Calculated equilibrium compositions during the hydrogen reduction of 1 kmol of WO_3 with initial hydrogen amounts of (a) 3, (b) 4, and (c) 5 kmol at a total pressure of 1 bar.

Accepted manuscript

For the MoO_3–H_2 system (Fig. 3), the reduction proceeds through the well-established two-step pathway:

$$MoO_3 + H_2(g) \rightarrow MoO_2 + H_2O(g) \quad (1)$$
$$MoO_2 + 2H_2(g) \rightarrow Mo + 2H_2O(g) \quad (2)$$

Therefore, MoO_2 represents the dominant intermediate over a broad temperature range before complete metallization.

Increasing the hydrogen amount progressively shifts the onset of metallic molybdenum formation from approximately 850 °C to about 700–750 °C while simultaneously increasing the final metallization degree.

The predicted two-step reduction sequence is fully consistent with the industrial hydrogen reduction process described by Habashi, where MoO_3 is first converted into MoO_2 and subsequently reduced to metallic molybdenum.[7] Similar reduction pathways have also been confirmed by recent in situ X-ray diffraction studies, which identified MoO_2 as the principal intermediate phase, whereas transient mixed-valence oxides represent kinetically controlled species not expected under equilibrium conditions.[9]

The W–O–H system exhibits a more complex reduction behavior (Fig. 4). In addition to WO_3, WO_2, and metallic W, several oxygen-deficient intermediate oxides, including $WO_{2.96}$, $WO_{2.90}$, and $WO_{2.72}$, were included in the Gibbs-energy minimization. These tungsten suboxides provide intermediate stages between WO_3 and WO_2 and account for the more gradual redistribution of oxygen during reduction. For clarity, only the principal phases are presented in the final equilibrium diagrams. In contrast to the comparatively simple MoO_3–MoO_2–Mo sequence, the distribution of tungsten among several oxide phases broadens the reduction interval and delays complete metallization. Similar observations have been reported for tungsten oxide reduction, where several suboxides may appear during hydrogen reduction depending on the experimental conditions.[9] However, the present equilibrium calculations indicate that WO_2 is the dominant thermodynamic intermediate, whereas other tungsten suboxides exhibit only minor equilibrium abundances.

Metallic tungsten begins to appear at approximately 800–850 °C for the stoichiometric mixture containing 3 kmol H_2. An increased hydrogen amount shifts its formation to slightly lower temperatures and increases the equilibrium metal yield. Nevertheless, even with 5 kmol H_2, complete reduction is not reached at 1500 °C. The calculated amounts of metallic W at this temperature are approximately 0.45, 0.65, and 0.87 kmol for initial hydrogen quantities of 3, 4, and 5 kmol, respectively. The remaining tungsten is distributed predominantly between WO_2 and small quantities of higher suboxides and residual WO_3.

A direct comparison of the two systems demonstrates that MoO_3 is more readily reduced to the metal than WO_3 under identical conditions. With 5 kmol H_2, essentially complete molybdenum metallization is achieved, whereas a measurable

Accepted manuscript

fraction of tungsten remains oxidized at 1500 °C. This difference agrees with the Ellingham analysis in Fig. 1, which showed that WO_3 has a more negative standard Gibbs energy of formation and is therefore thermodynamically more stable than MoO_3.

Despite these differences, both systems exhibit the same principal dependence on gas composition. Increasing the initial amount of hydrogen raises the equilibrium H_2/H_2O ratio, strengthens the reducing potential of the atmosphere, decreases the residual oxide content, and promotes metal formation. This explains why industrial extraction of Mo and W powders employs a continuous flow and excess of dry hydrogen, together with efficient removal of the generated water vapor.[9]

The effect of total pressure was also examined in additional calculations. Reducing the total pressure produced only negligible changes in the calculated equilibrium compositions. This is consistent with the overall reactions:

$$MoO_3+3H_2(g)=Mo+3H_2O(g) \quad (3)$$

$$WO_3+3H_2(g)=W+3H_2O(g) \quad (4)$$

for which the total number of gaseous moles remains unchanged. Accordingly, the equilibrium is controlled mainly by the ratio pH_2/pH_2O, rather than by the absolute total pressure. Since the equilibrium diagrams obtained at lower pressures were nearly identical, only the results calculated at 1 bar are presented.

Overall, the equilibrium calculations complement the standard Gibbs-energy analysis by showing that thermodynamic feasibility alone does not guarantee complete reduction. The attainable metal yield depends strongly on hydrogen excess and on the stability of intermediate oxides. The simpler Mo–O system permits nearly complete metallization under the investigated conditions, whereas the greater stability of WO_3 and the occurrence of multiple tungsten suboxides result in a broader reduction interval and a lower equilibrium yield of metallic tungsten. The principal equilibrium parameters characterizing the reduction of MoO_3 and WO_3 under different hydrogen amounts are summarized in Table I.

Accepted manuscript

TABLE I. Effect of the initial hydrogen amount on the equilibrium reduction of 1 kmol MoO_3 and WO_3 at 1500 °C and 1 bar.

Oxide	Initial H_2 / kmol	Approximate temp. of metal appearance / °C	Metal at 1500 °C / kmol	Principal residual oxide at 1500 °C	Approximate metallization degree [a] / %
MoO_3	3	850–900	0.50	MoO_2	50
MoO_3	4	750–800	0.82	MoO_2	82
MoO_3	5	700–750	≈1.00	Practically absent	≈100
WO_3	3	800–850	0.45	WO_2 + suboxides	45
WO_3	4	750–800	0.65	WO_2 + suboxides	65
WO_3	5	700–750	0.87	WO_2 + minor suboxides	87

[a]The metallization degree was calculated as the equilibrium amount of metallic Mo or W divided by the initial amount of the corresponding metal introduced as 1 kmol of MoO_3 or WO_3.

Thermodynamic analysis of the metallothermic reduction of V_2O_5

Fig. 5 compares the standard Gibbs free energy changes for the metallothermic reduction of vanadium pentoxide using aluminum, calcium, and magnesium over the investigated temperature range. All three reactions exhibit highly negative ΔG° values throughout the entire temperature interval, demonstrating that the reduction of V_2O_5 by these metallic reductants is thermodynamically feasible under standard conditions.

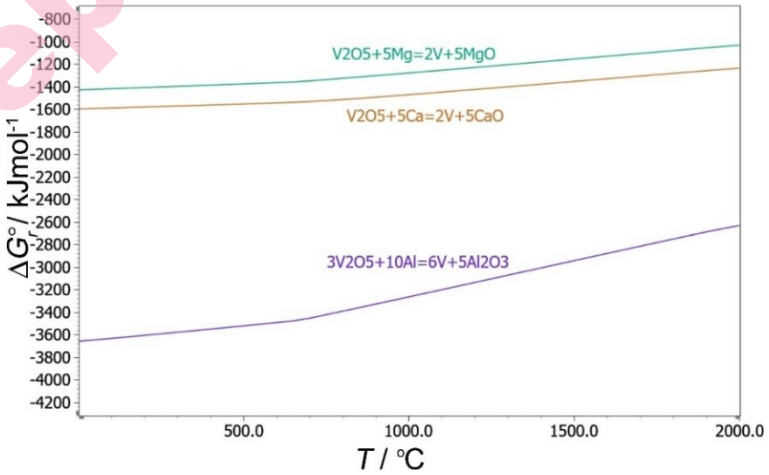


Fig. 5. Standard Gibbs free energy changes for the metallothermic reduction of vanadium pentoxide by aluminum, calcium, and magnesium as a function of temperature.

Accepted manuscript

Among the investigated reductants, aluminothermic reduction exhibits the most negative Gibbs free energy, indicating the largest thermodynamic driving force for oxygen removal from vanadium pentoxide. The high stability of Al_2O_3 makes aluminum the most effective reductant from a purely thermodynamic perspective. Calcium also shows very high reducing capability, although its driving force is somewhat lower than that of aluminum. Magnesium exhibits the least negative $\Delta G°$ values of the three reductants, but the reaction remains strongly spontaneous over the entire investigated temperature range.

For all three reactions, the Gibbs free energy becomes gradually less negative with increasing temperature, indicating a slight decrease in thermodynamic driving force. Nevertheless, the magnitude of $\Delta G°$ remains sufficiently negative even at 2000 °C, suggesting that thermodynamic limitations do not restrict the reduction process within the temperatures commonly employed in vanadium metallurgy.

These results indicate that the industrial selection of the reducing agent cannot be explained solely by thermodynamic considerations. Since aluminum, calcium, and magnesium all provide sufficient thermodynamic driving force for complete reduction, the preferred industrial route is governed primarily by technological and economic factors, including reaction controllability, reductant cost, product purity, by-product separation, and subsequent refining requirements.[10] Consequently, equilibrium calculations presented in the following part are necessary to evaluate the actual phase evolution and reduction behavior under practical processing conditions.

Fig. 6 shows the calculated equilibrium phase compositions during the reduction of 1 kmol V_2O_5 using stoichiometric amounts of aluminum, magnesium, and calcium at a total pressure of 1 bar. The initial reducing-agent amounts were defined according to the reactions:

$$3V_2O_5+10Al=6V+5Al_2O_3 \quad (5)$$

$$V_2O_5+5Mg=2V+5MgO \quad (6)$$

$$V_2O_5+5Ca=2V+5CaO \quad (7)$$

All relevant vanadium oxides were included in the Gibbs-energy minimization. Nevertheless, the calculated equilibrium compositions show that V_2O_5 is essentially completely converted into metallic vanadium over a broad temperature range for all three reducing agents. At 1200 °C, the equilibrium amounts closely approach the stoichiometric values of 2 kmol V together with 1.67 kmol Al_2O_3, 5 kmol MgO, or 5 kmol CaO, respectively. The negligible equilibrium amounts of intermediate vanadium oxides confirm that none of the investigated reactions is thermodynamically limited by the stability of VO_2, V_2O_3, or VO under these conditions.

Accepted manuscript

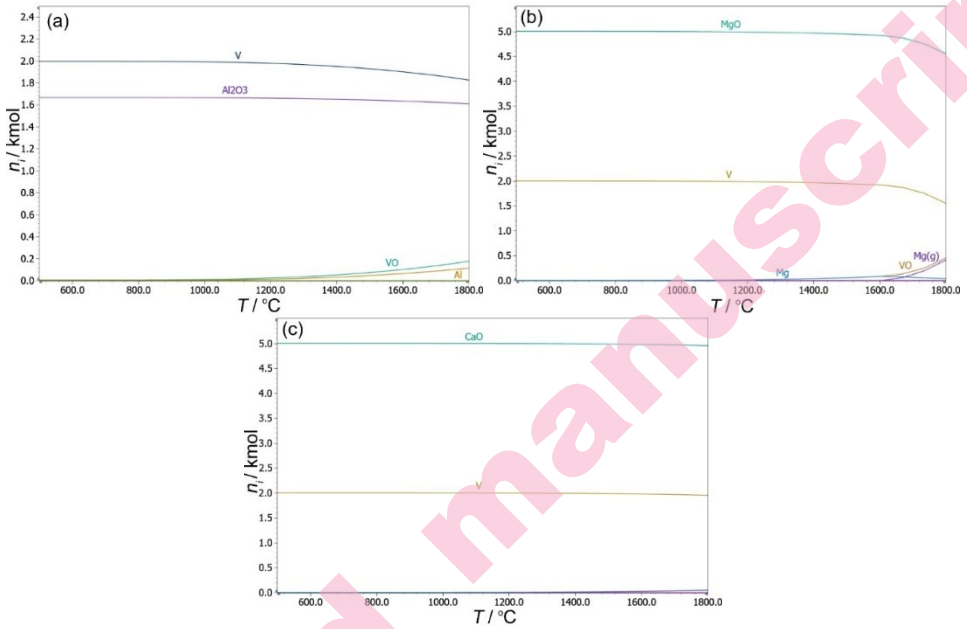


Fig. 6. Equilibrium phase compositions during the metallothermic reduction of 1 kmol V_2O_5 at 1 bar using stoichiometric amounts of (a) Al, (b) Mg, and (c) Ca.

For the aluminothermic system, metallic vanadium and Al_2O_3 remain the dominant products throughout most of the investigated temperature range. At very high temperatures, particularly above approximately 1400–1500 °C, a slight decrease in the equilibrium amounts of V and Al_2O_3 is accompanied by the appearance of small quantities of VO and residual Al. This behavior indicates partial reversal of the final reduction step and redistribution of oxygen between vanadium and aluminum-containing phases. The effect is suppressed when excess aluminum is introduced, although the thermodynamic improvement is accompanied by a considerable increase in the amount of residual Al. This result is consistent with the practical formation of crude V–Al products during aluminothermic extraction, which require subsequent dealuminization and refining.

The magnesiothermic system also exhibits essentially complete reduction at moderate temperatures. Under stoichiometric conditions, approximately 2 kmol V and 5 kmol MgO are stable up to around 1500–1600 °C. Above this range, the increasing volatility of magnesium becomes important. The equilibrium amount of Mg(g) increases, while the amounts of MgO and metallic V decrease and VO begins to form. The high-temperature redistribution may be represented schematically by:

$$V+MgO \rightleftharpoons VO+Mg(g) \quad (8)$$

Accepted manuscript

Therefore, although magnesium is an effective reducing agent, excessively high temperatures promote Mg volatilization, reductant loss, and partial reoxidation of vanadium. Calculations with 10 and 20% excess Mg showed that the additional reductant mainly remains as Mg or Mg(g), without substantially changing the vanadium metal yield in the technically relevant temperature range.

Calcium provides the most stable equilibrium products over the investigated interval. The calculated amounts of V and CaO remain very close to 2 and 5 kmol, respectively, even at elevated temperatures. In contrast to magnesium, appreciable calcium volatilization is predicted only near the upper end of the investigated range, while the formation of VO remains negligible. The results therefore confirm the exceptionally strong oxygen affinity of calcium and its ability to produce nearly complete vanadium metallization over a very broad temperature range. Excess calcium remains predominantly unreacted, with partial transfer to Ca(g) only at the highest temperatures.

The equilibrium calculations are consistent with the standard Gibbs-energy results, confirming that all three metallothermic reactions are strongly favorable. Within the thermodynamic equilibrium model implemented in HSC Chemistry, Al, Mg, and Ca all provide essentially complete reduction of V_2O_5 at 1200 °C. However, these predictions represent ideal equilibrium conditions and do not account for kinetic limitations or other factors affecting actual industrial processes. The practical differences between these reducing agents are therefore associated with high-temperature phase stability, reductant volatility, reaction control, product handling, and subsequent refining requirements. Although calcium is thermodynamically a very strong reducing agent and magnesium is also fully capable of reducing V_2O_5, aluminothermic reduction is the dominant commercial route. Aluminum is comparatively inexpensive, readily available, easy to store and handle, and substantially less volatile than magnesium. In addition, the aluminothermic reduction of V_2O_5 is highly exothermic, releasing sufficient heat to sustain an autogenous thermite process and facilitating its application on an industrial scale. Calcium reduction is more difficult to control because of its highly reactive nature, sensitivity to moisture, demanding storage requirements, and the violent character of the reaction. Magnesium introduces additional problems associated with evaporation, recovery of excess reductant, and separation of MgO from the metallic product. Consequently, the practical balance of thermodynamic effectiveness, cost, process controllability, scalability, and compatibility with subsequent vacuum or electron-beam refining explains why aluminothermic reduction remains the principal industrial route for producing crude vanadium. This agrees with the reviewed industrial practice, where aluminothermic reduction followed by vacuum treatment or electron-beam melting is identified as the mainstream route for high-purity vanadium production.[10]

Accepted manuscript

Thermodynamic analysis of halide-based extraction routes for Niobium and tantalum

Unlike molybdenum, tungsten, and vanadium, niobium and tantalum are not commonly produced by direct reduction of their oxides because of the very high thermodynamic stability of Nb_2O_5 and Ta_2O_5. Instead, industrial production is predominantly based on halide intermediates, in which the refractory oxides are first converted into volatile pentachlorides or fluoride complexes, followed by metallothermic reduction to the corresponding metals.[7] This approach not only overcomes the high stability of the oxides but also enables efficient purification and separation of niobium and tantalum, whose chemical properties are otherwise very similar. Consequently, chlorination and carbochlorination represent key thermodynamic steps in the industrial extraction of these refractory metals.

To evaluate the thermodynamic driving force of the chlorination process, the standard Gibbs free energy changes for direct chlorination and carbochlorination of Nb_2O_5 and Ta_2O_5 were calculated and are presented in Fig. 7.

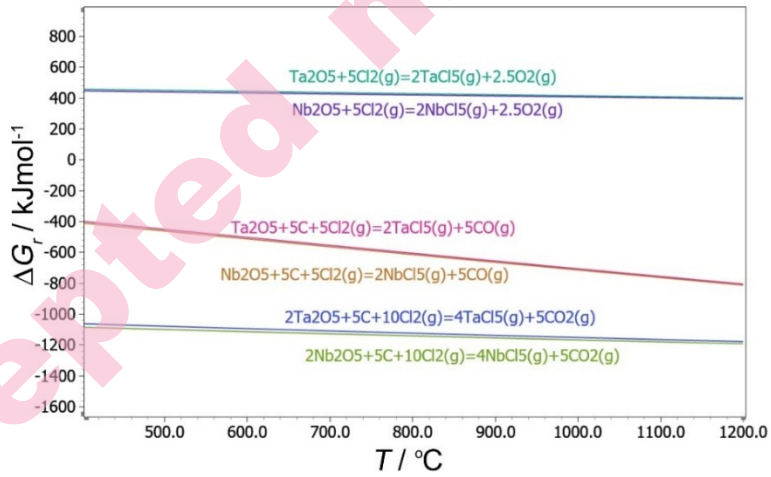


Fig. 7. Standard Gibbs free energy changes for direct chlorination and carbochlorination of Nb_2O_5 and Ta_2O_5.

Fig. 7 clearly demonstrates that direct chlorination of Nb_2O_5 and Ta_2O_5 is thermodynamically unfavorable over the entire investigated temperature range. The calculated Gibbs free energy changes remain strongly positive, approximately +400–450 kJ, indicating that chlorine alone cannot effectively convert the refractory oxides into volatile pentachlorides. A completely different thermodynamic behavior is obtained when carbon is introduced as an auxiliary reducing agent. Both carbochlorination reactions leading to the formation of CO exhibit strongly negative Gibbs free energy changes throughout the investigated temperature range, confirming that simultaneous reduction and chlorination efficiently destabilize the oxide lattice and promote the formation of volatile

Accepted manuscript

$NbCl_5(g)$ and $TaCl_5(g)$. The driving force becomes even larger when carbon is completely oxidized to CO_2, where $\Delta G°$ decreases to approximately –1100 to –1200 kJ. These results demonstrate that the removal of oxygen as carbon oxides is the principal thermodynamic factor responsible for the feasibility of the chlorination process.

Only relatively small differences are observed between niobium and tantalum. In all corresponding reactions, Ta_2O_5 exhibits slightly less negative Gibbs free energy changes than Nb_2O_5, indicating its somewhat higher thermodynamic stability. Nevertheless, the differences are modest and both oxides exhibit essentially the same extraction behavior. Consequently, the choice of operating conditions in industrial practice is governed primarily by process kinetics, separation requirements, and purification considerations rather than by significant differences in equilibrium thermodynamics.

The calculated thermodynamic trends are consistent with the industrial extraction route described by Habashi[7] and the chlorination studies of niobium and tantalum oxides reported by Allain et al.[11] Industrial production of niobium and tantalum involves purification and separation of Nb_2O_5- and Ta_2O_5-containing concentrates, followed by reductive chlorination in the presence of carbon at approximately 900 °C to produce volatile $NbCl_5$ and $TaCl_5$, while oxygen is removed as CO. The present calculations quantitatively support this process by showing that only carbochlorination provides a sufficiently large thermodynamic driving force for pentachloride formation, whereas direct chlorination remains unfavorable over the investigated temperature range. These findings are further supported by the equilibrium calculations and experimental results of Yang and Hlavacek, who reported complete conversion of both Nb_2O_5 and Ta_2O_5 in the presence of chlorine and carbon (or CO), with $NbCl_5$ and $TaCl_5$ as the principal products.[12] Their results also confirmed that direct chlorination is insignificant and that both oxides exhibit very similar equilibrium behavior, consistent with the small differences between the corresponding $\Delta G°$ curves obtained in the present study.

Although the reactions producing CO_2 exhibit a larger standard thermodynamic driving force, their equilibrium simulations showed that CO becomes the dominant carbon-containing product above approximately 800 °C. Therefore, the reaction $M_2O_5+5C+5Cl_2(g)=2MCl_5(g)+5CO(g)$ is expected to dominate within the industrially relevant temperature range of 800–1000 °C.

Fig. 8 presents the standard Gibbs free energy changes for the reduction of gaseous niobium and tantalum pentachlorides by hydrogen, sodium, magnesium, and calcium. All reactions were normalized to one mole of the corresponding pentachloride, enabling direct comparison of the thermodynamic driving forces associated with the investigated reducing agents.

Accepted manuscript

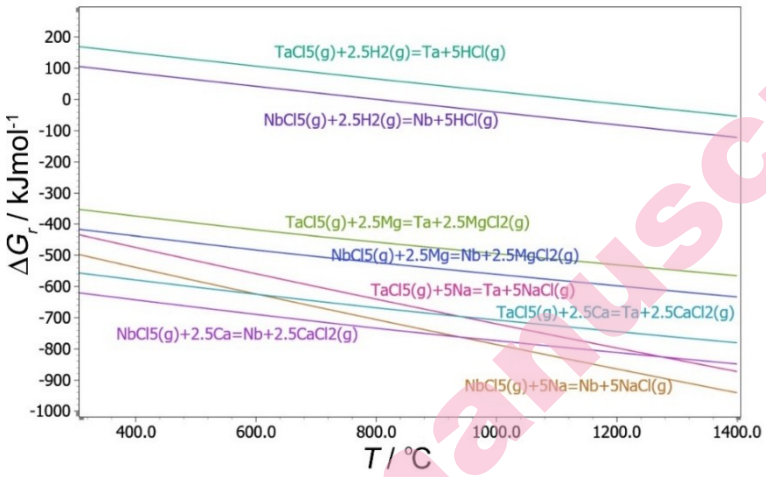


Fig. 8. Standard Gibbs energy changes for the reduction of $NbCl_5$ and $TaCl_5$ by H_2, Na, Mg, and Ca. All reactions were normalized to one mole of pentachloride.

The calculated results reveal a clear distinction between hydrogen reduction and metallothermic reduction. Reactions involving Na, Mg, and Ca exhibit strongly negative Gibbs free energy values throughout the entire investigated temperature range, confirming that all three metallic reductants are thermodynamically capable of converting $NbCl_5$ and $TaCl_5$ into the corresponding metals. In contrast, the overall hydrogen-reduction reactions are unfavorable at lower temperatures and become thermodynamically feasible only after a critical temperature is exceeded.

For each reducing agent, reduction of $NbCl_5$ is more favorable than reduction of $TaCl_5$. The difference is particularly pronounced for hydrogen. The overall reaction:

$$NbCl_5(g)+2.5H_2(g)=Nb+5HCl(g) \quad (9)$$

becomes thermodynamically favorable at a substantially lower temperature than the corresponding $TaCl_5$ reaction. According to the calculated trends, complete hydrogen reduction of $NbCl_5$ becomes feasible at approximately 750–800 °C, whereas $TaCl_5$ requires temperatures of roughly 1100–1200 °C. This confirms the greater resistance of tantalum pentachloride toward hydrogen reduction and indicates that higher temperature and a larger H_2/HCl ratio are required for tantalum production.

The overall hydrogen-reduction curves provide a simplified representation of the net conversion to metal. In practice, hydrogen reduction proceeds stepwise through lower chlorides and disproportionation reactions rather than by a single direct reaction. Experimental studies of $NbCl_5$ reduction have shown that the reaction begins near 400 °C.[17] At approximately 400–550 °C, $NbCl_5$ is first

Accepted manuscript

reduced to $NbCl_4$, followed by formation of lower chlorides, particularly Nb_3Cl_8. Metallic niobium begins to appear above about 600 °C, while high metal yields require temperatures above approximately 1000 °C. Under optimized conditions at 1200 °C, niobium yields close to 95% were reported.[17] The intermediate reactions were omitted from Figure 8 to preserve graphical clarity, but their contribution must be considered when interpreting the hydrogen route. The calculated overall $\Delta G°$ curve therefore defines the limiting thermodynamic tendency for complete conversion, whereas the experimentally observed reaction pathway is controlled by the stability and disproportionation behavior of lower niobium chlorides.

The metallothermic reactions display much larger negative Gibbs free energy values than the hydrogen reactions. This reflects the strong stability of NaCl, $MgCl_2$, and $CaCl_2$ and confirms that reduction of the pentachlorides by active metals is not significantly limited by equilibrium thermodynamics. The relative ranking of the metallic reducing agents varies with temperature because of differences in reaction entropy and the thermodynamic properties of the corresponding chloride products. Consequently, the most negative curve at a particular temperature should not be interpreted as the sole criterion for industrial selection.

Sodium reduction becomes particularly favorable at elevated temperatures, especially for $NbCl_5$, while calcium provides a very large thermodynamic driving force over much of the investigated range. Magnesium also remains strongly favorable and exhibits a comparatively regular temperature dependence. In practical terms, however, the selection among Na, Mg, and Ca is governed by additional factors, including reductant cost, reaction intensity, handling safety, contamination risk, volatility, salt separation, and the possibility of recovering or removing the by-product chlorides.

Overall, the results demonstrate that metallothermic reduction is thermodynamically more robust than hydrogen reduction for both $NbCl_5$ and $TaCl_5$. Hydrogen remains technologically attractive because it avoids introducing metallic impurities and solid reducing-agent residues, but it requires elevated temperatures, excess hydrogen, continuous removal of HCl, and careful control of multiple intermediate chloride reactions. Metallothermic routes are therefore more suitable for bulk metal production, whereas hydrogen reduction is more strongly dependent on process design and may be particularly useful in specialized high-purity or vapor-phase applications.

CONCLUSION

a) Ellingham analysis demonstrates that Nb_2O_5 and Ta_2O_5 possess the highest thermodynamic stability among the investigated refractory-metal oxides, whereas

Accepted manuscript

MoO_3 and WO_3 are considerably less stable and therefore more amenable to hydrogen reduction.

b) The exceptionally high stability of Nb and Ta carbides provides an additional thermodynamic explanation for the limited applicability of carbothermic reduction.

c) Equilibrium calculations show that hydrogen reduction of MoO_3 proceeds through the MoO_2 intermediate and is strongly promoted by hydrogen excess, while the more complex W–O system exhibits a broader reduction interval because of the formation of tungsten suboxides.

d) Al, Mg, and Ca are all thermodynamically capable of reducing V_2O_5, but industrial preference for aluminothermy results primarily from technological and economic advantages rather than equilibrium limitations.

e) Direct chlorination of Nb_2O_5 and Ta_2O_5 is thermodynamically unfavorable, whereas carbochlorination provides a large thermodynamic driving force for the formation of volatile pentachlorides.

f) Overall, the results demonstrate how differences in oxide and carbide stability and reduction behavior influence the selection of industrial extraction routes for refractory metals.

The present analysis is based on equilibrium thermodynamics and therefore does not account for kinetic limitations, mass-transfer phenomena, reactor design, or process economics, which should be considered during industrial process optimization.

Acknowledgements: The research presented in this paper was done with the financial support of the Ministry of Science, Technological Development and Innovations of the Republic of Serbia, within the funding of the scientific research work at the University of Belgrade, Technical Faculty in Bor, according to the contract with registration number 451-03-34/2026-03/20013.

И З В О Д

ТЕРМОДИНАМИЧКА АНАЛИЗА ИНДУСТРИЈСКИХ ПИРОМЕТАЛУРШКИХ ПОСТУПАКА ЕКСТРАКЦИЈЕ ВАТРОСТАЛНИХ МЕТАЛА

ДРАГАН МАНАСИЈЕВИЋ

Универзитет у Београду, Технички факултет у Бору, Бор, Србија.

Индустријска производња ватросталних метала првенствено је условљена термодинамичким ограничењима која произилазе из великог афинитета ових метала према угљенику и кисеонику. У овом раду спроведена је обједињена термодинамичка анализа репрезентативних ватросталних метала (V, Nb, Ta, Mo, W и Re) са циљем утврђивања термодинамичке основе за избор пирометалуршких поступака екстракције. За поређење стабилности оксида, склоности ка образовању карбида, редукције водоником, металотермијске редукције и поступака екстракције заснованих на хлоровању примењени су прорачуни стандардне Гибсове енергије, Елингамови дијаграми и равнотежни прорачуни у програму HSC Chemistry. Прорачуни показују да Nb_2O_5 и Ta_2O_5 поседују највећу

Accepted manuscript

термодинамичку стабилност и истовремено најизраженију склоност ка образовању карбида, што објашњава зашто се у индустрији предност даје хлоровању праћеном металотермијском редукцијом. Насупрот томе, MoO_3 и WO_3 могу се довољно ефикасно редуковати водоником, док равнотежни прорачуни указују на значајан утицај вишка водоника на коначни степен метализације. Металотермијска редукција V_2O_5 помоћу Al, Mg и Ca термодинамички је могућа у испитиваном температурном опсегу, док је индустријска предност алуминотермије углавном одређена технолошким и економским факторима. Термодинамичка анализа хлоровања и карбохлоровања додатно показује да је директно хлоровање Nb_2O_5 и Ta_2O_5 неповољно, док карбохлоровање обезбеђује велику покретачку силу за образовање пентахлорида. Добијени резултати пружају доследно термодинамичко објашњење избора индустријских поступака екстракције ватросталних метала.

(Примљено 21. августа; ревидирано 6. новембра; прихваћено 9. новембра 2026.)

REFERENCES

1. C. Ma, Y. Gui, Y. Wang, X. Dong, Y. Huang, H. Fu, G. Shu, *J. Mater. Eng. Perform.* **34** (2025) 7265–7287 (https://dx.doi.org/10.1007/s11665-024-10566-8)
2. B. Liu, P. Zhang, H. Yan, Q. Lu, H. Shi, Z. Liu, D. Wu, T. Sun, R. Li, Q. Wang, *J. Mater. Eng. Perform.* **33** (2024) 9945–9975 (https://dx.doi.org/10.1007/s11665-024-09693-z)
3. J. Wittenauer, K. Liddell, *JOM* **43** (1991) 6–7 (https://dx.doi.org/10.1007/BF03220612)
4. W. Knabl, G. Leichtfried, R. Stickler, Refractory Metals and Refractory Metal Alloys, in Springer Handbook of Materials Data, H. Warlimont, W. Martienssen, Eds., Springer, Cham, Switzerland, 2018, pp. 307–337 (https://dx.doi.org/10.1007/978-3-319-69743-7_13)
5. M. Y. Araghi, A. Dashti, M. Fani, I. Ghamarian, C. Ruiz, S. Xu, *J. Mater. Res. Technol.* **37** (2025) 870–892 (https://doi.org/10.1016/j.jmrt.2025.05.207)
6. M. G. Haile, A. Oladunni Oyelola, F. Olufemi Aramide, S. Ojo Seidu, O. Akinlabi, *Miner. Process. Extr. Metall.* **134** (2025) 3–12 (https://dx.doi.org/10.1177/25726641241301982)
7. F. Habashi, Precious Metals, Refractory Metals, Scattered Metals, Radioactive Metals, Rare Earth Metals, Vol. 3, in Handbook of Extractive Metallurgy, F. Habashi, Ed., Wiley-VCH, Weinheim, Germany, 1997.
8. Y. Chen, R. Yang, C. Zhang, J. Song, Y. Che, J. He, *Int. J. Refract. Met. Hard Mater.* **106** (2022) 105869 (https://dx.doi.org/10.1016/j.ijrmhm.2022.105869)
9. M. Häger, S. Keilholz, H. Kohlmann, *Eur. J. Inorg. Chem.* **28** (2025) e202500089 (https://dx.doi.org/10.1002/ejic.202500089)
10. R. Yuan, S. Li, Y. Che, J. He, J. Song, B. Yang, *Int. J. Refract. Met. Hard Mater.* **101** (2021) 105696 (https://dx.doi.org/10.1016/j.ijrmhm.2021.105696)
11. E. Allain, M. Djona, I. Gaballah, *Metall. Mater. Trans. B* **28** (1997) 223–233 (https://dx.doi.org/10.1007/s11663-997-0088-1)
12. F. Yang, V. Hlavacek, *AIChE J.* **45** (1999) 581–589 (https://dx.doi.org/10.1002/aic.690450315)
13. A. Roine, HSC Chemistry, Version 10.8.0.6, Metso, Pori, Finland, 2026.
14. L. Backman, E. J. Opila, *J. Eur. Ceram. Soc.* **39** (2019) 1796–1802 (https://dx.doi.org/10.1016/j.jeurceramsoc.2018.11.004)

Accepted manuscript

15. L. *Shen*, F. Tesfaye, X. Li, D. Lindberg, P. Taskinen, *Miner. Eng.* **161** (2021) 106719 (https://doi.org/10.1016/j.mineng.2020.106719)
16. C. R. Weinberger, G. B. Thompson, *J. Am. Ceram. Soc.* **101** (2018) 4401–4424 (https://dx.doi.org/10.1111/jace.15768)
17. Y. Saeki, T. Suzuki, *J. Electrochem. Soc. Jpn.* **33** (1965) 220–228 (https://dx.doi.org/10.5796/jesj.33.4.220).

Accepted manuscript